Green Chemistry

PAPER

View Article Online
View Journal | View Issue

Cite this: *Green Chem.*, 2014, **16**, 1236

Lignin fate and characterization during ionic liquid biomass pretreatment for renewable chemicals and fuels production†

Noppadon Sathitsuksanoh,[a] Kevin M. Holtman,[b] Daniel J. Yelle,[c] Trevor Morgan,[d] Vitalie Stavila,[e] Jeffrey Pelton,[f] Harvey Blanch,[a,g] Blake A. Simmons[a,e] and Anthe George*[a,e]

The fate of lignin from wheat straw, Miscanthus, and Loblolly pine after pretreatment by a non-toxic and recyclable ionic liquid (IL), [C_2mim][OAc], followed by enzymatic hydrolysis was investigated. The lignin partitioned into six process streams, each of which was quantified and analyzed by a combination of a novel solution-state two-dimensional (2D) nuclear magnetic resonance (NMR) method, and size exclusion chromatography (SEC). Pretreatment of biomass samples by [C_2mim][OAc] at 120 and 160 °C enhances hydrolysis rates and enzymatic glucan digestions compared to those of untreated biomass samples. Lignin partitioning into the different streams can be controlled by altering the ionic liquid pre-treatment conditions, with higher temperatures favoring higher lignin partitioning to the IL stream. 2D NMR bond abundance data and SEC results reveal that lignin is depolymerized during ionic liquid pretreatment, and lignin of different molecular masses can be isolated in the different process streams. SEC suggested that higher molecular mass lignin was precipitated from the ionic liquid, leaving smaller molecular mass lignin in solution for further extraction. Lignin obtained as a residue of enzymatic hydrolysis contained the highest molecular mass molecules, similar in structure to the control lignin. The results suggest that isolated lignins *via* IL pretreatment from all three feedstocks were both depolymerized and did not contain new condensed structures. This finding leads to the possibility that lignin obtained from this IL pretreatment process may be more amenable to upgrading, thereby enhancing biorefinery economics.

Received 7th November 2013,
Accepted 18th November 2013

DOI: 10.1039/c3gc42295j

www.rsc.org/greenchem

1. Introduction

Currently, most liquid transportation fuels are derived from crude oil. An increase in gasoline demand with a limited crude oil supply makes lignocellulosic biofuels from non-food feedstocks an attractive solution to displace a significant amount of gasoline.[1] Lignocellulosic biomass consists of associated networks of carbohydrates and lignin. The carbohydrate fraction in lignocellulosic biomass can be hydrolyzed to monomeric sugars, which can be fermented into biofuels. However, lignocellulose is naturally resistant to chemical and biological disturbances (*e.g.*, fungal decay and their associated enzymatic and non-enzymatic pathways), in turn making it difficult to release sugars from the recalcitrant lignin structure. For bioconversion of biomass, pretreatment is necessary to enhance substrate accessibilities and achieve high sugar yields, whilst minimizing the use of costly enzymes.

Cellulose solvent-based lignocellulose pretreatments have gained attention because they can increase substrate accessibility to hydrolytic enzymes more effectively than traditional pretreatments. As a result, hydrolysis rates and the glucan digestibility of pretreated biomass are increased and enzyme use decreased.[2–6] Moreover, ionic liquids have been shown to be excellent pretreatment solvents irrespective of the type of biomass feedstock.[7–11] Additionally, lignin can be extracted from lignocellulose *via* ionic liquid pretreatment without high

[a]*Joint BioEnergy Institute, 5885 Hollis St., Emeryville, CA 94608, USA. E-mail: ageorge@lbl.gov*
[b]*U.S. Department of Agriculture, Agricultural Research Services, Western Regional Research Center, Bioproduct Chemistry and Engineering Research, Albany, CA 94710, USA*
[c]*U.S. Forest Service, Forest Products Laboratory, Madison, WI, USA*
[d]*Hawaii Natural Energy Institute, University of Hawaii, USA*
[e]*Sandia National Laboratories, Livermore, CA, USA*
[f]*Physical Biosciences Division, Lawrence Berkeley National Laboratory, 1 Cyclotron Rd, Berkeley, CA 94720, USA*
[g]*Department of Chemical and Biomolecular Engineering, University of California, Berkeley, CA 94720-1462, USA*
†Electronic supplementary information (ESI) available. See DOI: 10.1039/c3gc42295j

energy consumption. To date, many ionic liquids have been synthesized and effectively used as cellulose solvents for pretreatment, although their toxicity as biorefinery solvents have yet to be assessed. Recently the IL [C_2mim][OAc] has been granted a discharge permit at the DOE funded Advanced Biofuels Demonstration Unit at concentrations <28.8% due to its lack of fish toxicity at these concentrations.‡§ A previous study has shown that sugar hydrolysates after pretreatment by [C_2mim][OAc] did not affect downstream biocatalytic conversion of pretreated switchgrass to free fatty acids.[12] Additionally, [C_2mim][OAc] has been shown to be recyclable[13] giving scope for its use in an environmentally and economically feasible biorefinery process. Due to these attributes, [C_2mim][OAc] was chosen as the pretreatment solvent in this study.

The effectiveness of [C_2mim][OAc] as a pretreatment solvent is partly due to its ability to disrupt lignin. Lignin is a complex biopolymer derived from three basic monolignols (*p*-coumaryl, coniferyl, and sinapyl alcohols), and typically constitutes 15–30% of the feedstock. With projected biorefinery output, a substantial amount of residual lignin will be available. During pretreatment and enzymatic hydrolysis steps, most lignin can be separated and ends up as a waste stream. Feedstock cost accounts for one-third of the total production cost of cellulosic ethanol.[14] Consequently, production of value-added products from lignin would improve the process economics, and contribute to new renewable sources of petroleum derived materials.

In order to efficiently extract and eventually use lignin, we must understand both its partitioning into the different streams of the biofuels operation and also its chemical composition and how pretreatment affects its chemical structure. Although the chemical structure of lignin has not been comprehensively understood, lignin monomers are believed to be connected by a variety of bonds, such as carbon–oxygen bonds (*e.g.*, β-O-4, α-O-4) and carbon–carbon bonds (*e.g.*, β–β, β-5, and 5–5).

The lignin macromolecule is heterogeneous in nature and contains a variety of functional groups that have an impact on its reactivity. Pretreatment steps in biochemical conversion of biomass can simultaneously depolymerize and repolymerize lignin, increasing the degree of heterogeneity of the resulting lignin and negatively affecting its solubility and reactivity.[15] The use of harsh chemicals, high temperatures, and/or long pretreatment times during biomass conversion is usually accompanied by an increase in lignin condensation. A decrease in the number of β-O-4 linkages, which are fragmented and possibly recondensed, is also observed,[16–18] depending on the pretreatment method. Residual lignins obtained from such processes are challenging to catalyze, which limits the possibilities to enhance their properties.[19] Consequently, due to lack of understanding of changes in the chemical structure of lignin from pretreatment, potential uses for lignin are limited.

‡BC Laboratories Inc., Bekrsfield, CA 93308, USA.
§J. M. Polisini and R. G. Miller, California Department of Fish and Game, Sacramento, CA, 1988.

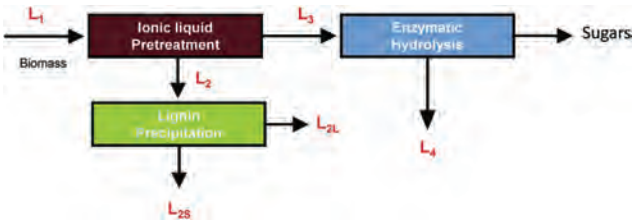

Fig. 1 Schematic diagram of extracted lignin from different streams during IL pretreatment and enzymatic hydrolysis. L_1: lignin from untreated biomass, L_2: solubilized lignin in [C_2mim][OAc], L_{2S}: precipitated solid lignin from L_2, L_{2L}: remaining lignin in the supernatant after L_{2S} precipitation, L_3: lignin in pretreated biomass, and L_4: lignin remaining after enzymatic hydrolysis.

In this work we conduct a complete mass balance analysis during ionic liquid pretreatment with [C_2mim][OAc], for carbohydrates and lignin from wheat straw, Miscanthus, and Loblolly pine followed by enzymatic hydrolysis (Fig. 1). Extracted lignin from different feedstocks under different extraction conditions was characterized by a novel two-dimensional (2D) ^{13}C–^{1}H heteronuclear single quantum coherence (HSQC) nuclear magnetic resonance (NMR) method for extensive structural feature determination. Size exclusion chromatography (SEC) was employed to understand relative polydispersity changes in the different process streams. The results provide insight into the chemical structure and size of lignin polymers from different biomass types, and during IL pretreatment and enzymatic hydrolysis.

2. Materials and methods

2.1. Chemicals and materials

All chemicals were reagent grade and purchased from Sigma-Aldrich (St. Louis, MO), unless otherwise noted. 1-Ethyl-3-methylimidazolium acetate, [C_2mim][OAc], was purchased from BASF 98% purity lot no. 11-0005 and used as received. The *Trichoderma reesei* cellulase (Ctec 2) was given by Novozymes North America (Franklinton, NC), containing 188 mg protein per mL. Miscanthus and wheat straw samples were procured from the Energy Bioscience Institute and University of Toledo, respectively. Loblolly pine wood samples were provided by ArborGen (Summerville, SC). The air-dried biomass was milled by a Thomas-Wiley Mini Mill fitted with a 40-mesh screen (Model 3383-L10 Arthur H. Thomas Co., Philadelphia, PA, USA) and sieved to the nominal sizes of 40–60 mesh (250–400 μm). All feedstocks were further dried in the vacuum oven at 40 °C overnight prior to pretreatment to eliminate the variable of moisture content.

2.2. Isolation of enzymatic mild acidolysis lignin (EMAL)

Ball-milling of biomass was performed using a Retsch PM 100 planetary ball mill spinning at 600 rpm with zirconium dioxide (ZrO_2) container and balls. The ball milling conditions

were described elsewhere.[20] Briefly, the ball-milled biomass samples were treated with cellulase (Ctec 2) and hemicellulase (Htec 2) in the amount of 50 mg protein per g biomass. The enzymatic hydrolysis was carried out at 50 °C for 48 h at 2% consistency in the presence of 2% Tween 20 in 50 mM citrate buffer (pH ~ 4.8). The insoluble materials were washed with deionized water and a fresh batch of enzymes, in the same quantity, was added for another 48 h. The insoluble materials remaining after enzymatic hydrolysis were washed with deionized water to remove soluble sugars. Residual proteins on the surface of solid pellets were then washed twice with 6 M guanidine hydrochloride (Gnd HCl) and freeze dried. The crude lignin obtained was further subjected to mild acid hydrolysis using an azeotrope of dioxane–water (96 : 4 (v/v)) containing 0.01 N HCl under nitrogen atmosphere. The resulting suspension was centrifuged, and the supernatant was collected. The supernatant was neutralized with 2 M sodium bicarbonate and then added drop-wise into 1 L acidified water (pH 2.0). The precipitated lignin was allowed to equilibrate overnight, recovered by centrifugation, washed with deionized water twice, and freeze dried.

2.3. Ionic liquid pretreatment

Ionic liquid pretreatment of lignocellulose was conducted on wheat straw, Miscanthus, and Loblolly pine. Briefly, 15% (w/w) biomass in [C_2mim][OAc] was loaded in a Syrris globe reactor at 120 and 160 °C for 90 min, unless otherwise noted. The hydrogel-like solution was allowed to cool to 50 °C. Recovery methods and mass balances for four lignin streams are described in the Mass balance section.

2.4. Mass balance

Mass balance diagrams for pretreatment by [C_2mim][OAc] at 120 and 160 °C and enzymatic hydrolysis based on 100 g of dry biomass were constructed. The overall and enzymatic glucose and xylose yields were determined from pretreatment and enzymatic hydrolysis. Fig. 1 shows the fate of lignin during the course of pretreatment and enzymatic hydrolysis. Four solid lignin streams and three liquid lignin streams were defined and characterized. Notation "L_x" was used throughout to represent lignin from different streams. Solid lignin from untreated biomass was denoted as L_1. To date, there is no ideal lignin extraction method that can extract lignin whilst simultaneously maintaining its native structural integrity and removing all carbohydrates. As such, it is very difficult to definitively characterize changes of lignin due to extraction processes based on a robust lignin control. In the present study, enzymatic mild acid lignin (EMAL) of each feedstock was used to, as much as possible, represent the 'native' lignin in the biomass (denoted as L_1, Fig. 1). However it should be noted that this lignin does contain small quantities of carbohydrates and some linkages might be lost due to ball milling and the addition of small quantities of HCl during the extraction procedure. During IL pretreatment, lignocellulose was solubilized and the dissolved lignin fraction in the IL after pretreatment was denoted as L_2. Pretreated biomass in L_3 was obtained after adding an organic precipitant (*i.e.* 1 : 1 acetone–water (v/v)). Acetone was removed from this stream by evaporation, and excess water was added. The precipitated biomass is filtered. The supernatant was refrigerated overnight. Solid precipitate (denoted as L_{2S}) was recovered by centrifugation, washed with water twice, and freeze dried. The liquid fraction after L_{2S} precipitation was denoted as L_{2L}. Unextracted lignin that remained in pretreated biomass was denoted as L_3, which can be extracted after enzymatic hydrolysis, denoted as L_4.

2.5. Carbohydrate assay

The carbohydrate composition of biomass prior to pretreatment and residual biomass after hydrolysis were determined with a modified quantitative saccharification (QS) procedure.[21] In the modified QS, secondary hydrolysis was conducted in the presence of 1% (w/w) sulfuric acid at 121 °C for 1 h to more accurately determine the quantities of sugars susceptible to acid degradation (*e.g.*, xylan). After $CaCO_3$ neutralization and centrifugation, monomeric sugars in the supernatant were measured with an Agilent HPLC equipped with a Bio-Rad Aminex HPX-87P column (Richmond, CA) at a rate of 0.6 mL of deionized water per min at 60 °C.

2.6. Lignin and ash assays

The standard NREL biomass protocol was used to measure lignin and ash.[22] Briefly, solids remaining after two-stage acid hydrolysis were held at 105 °C overnight. The mass of the dried solids corresponds to the amount of acid-insoluble lignin and ash in the sample. The mass of the ash only fraction was then determined by heating the solids to 575 °C for 24 h. Percent acid-soluble lignin in the sample was determined by measuring the UV absorption of the acid hydrolysis supernatant at 320 nm. All carbohydrate and lignin assays were conducted in triplicate.

2.7. Enzymatic hydrolysis

The pretreated samples were diluted to 10 g glucan per liter in a 50 mM sodium citrate buffer (pH 4.8) supplemented with 0.1% (w/v) NaN_3, which prevented the growth of microorganisms. All enzymatic hydrolysis experiments were conducted in triplicate. Pretreated samples were completely suspended in a rotary shaker at 250 rpm at 50 °C. The enzyme loadings were 20 mg protein (Ctec 2) per gram of glucan. Eight hundred microliters of well-mixed hydrolysate were removed, followed by immediate centrifugation at 13 000 rpm for 5 min. Exactly 500 μL of the supernatant was transferred to another microcentrifuge tube and stayed at room temperature for 30 min, to allow the conversion of all cellobiose to glucose. The supernatant was then acidified by adding 30 μL of 10% (w/w) sulfuric acid, followed by freezing overnight. The frozen samples were thawed, mixed well, and then centrifuged at 13 000 rpm for 5 min, to remove any precipitated solid sediments. The soluble glucose and xylose in the enzymatic hydrolysate were measured by HPLC equipped with a Bio-Rad HPX-87H column at a rate of 0.6 mL of 0.1% (v/v) sulfuric acid per min at 60 °C. Galactose and mannose co-eluted with xylose. As such, for

pine samples, a Bio-Rad HPX-87P column at a rate of 0.6 mL of deionized water per min at 80 °C was used. After 72 h hydrolysis, the remaining hydrolysate was transferred to a 50 mL centrifuge tube, centrifuged at 4500 rpm for 15 min, and soluble sugar content was determined using the same procedure as other hydrolysate samples, as described above. After all remaining hydrolysate was decanted, the pellets were resuspended in 20 mL of water and centrifuged to remove residual soluble sugars from the pellets. The sugar content of the washed pellets was determined by modified QS as described above. Enzymatic glucan digestibility after 72 h was calculated using the ratio of soluble glucose in the supernatant to the sum of this soluble glucose and the glucose equivalent of the residual glucan.

2.8. X-ray diffraction (XRD)

The XRD experiments were performed on a PANalytical Empyrean X-ray diffractometer equipped with a PIXcel^{3D} detector and operated at 45 kV and 40 kA using Cu Kα radiation (λ = 1.5418 Å). The patterns were collected in the 2θ range from 5 to 55° with the step size of 0.026° and the exposure time of 300 seconds. A reflection-transmission spinner was used as a sample holder and the spinning rate was set at 8 rpm throughout the experiment. All spectra were subjected to baseline correction using PeakFit1 4.12 software (Systat Software Inc., Chicago, IL) assuming Gaussian distribution function as the shape of the resolved peaks and Saviszky–Golay smoothing.[4] The crystallinity index (CrI) was determined by Segal method.[23]

2.9. 2D ^{13}C–^{1}H HSQC NMR spectroscopy

Plant cell wall samples were extracted to remove extractives and ball milled as previously described.[20,24] The milled samples (~50 mg) were then placed in NMR tubes with 600 μL DMSO-d_6 using a minute amount of [C_2mim][OAc] as a co-solvent.[25] The samples were sealed and sonicated until homogenous in a Branson 2510 table-top cleaner (Branson Ultrasonic Corporation, Danbury, CT). The temperature of the bath was closely monitored and maintained below 55 °C. Lignin samples were added to 600 μL DMSO-d_6 and sonicated until homogenous. The homogeneous lignin solutions were transferred to NMR tubes. HSQC spectra were acquired at 25 °C using a Bruker Avance-600 MHz instrument equipped with a 5 mm inverse-gradient ^{1}H/^{13}C cryoprobe using a q_hsqcetgp pulse program (ns = 200 for cell wall and 64 for lignin, ds = 16, number of increments = 256, d_1 = 1.0 s).[26] Chemical shifts were referenced to the central DMSO peak (δ_C/δ_H 39.5/2.5 ppm). Assignment of the HSQC spectra was described elsewhere.[20,27] A semi-quantitative analysis of the volume integrals of the HSQC correlation peaks was performed using Bruker's Topspin 3.1 (Windows) processing software. A cosine squared function was applied to both F_2 (LB = −0.05, GB = 0.001) and F_1 (LB = −0.01, GB = 0.001) prior to 2D Fourier transformation. Semi-quantitative evaluation of interunit linkages in lignins has been typically expressed as number of specific interunit linkages per 100 aromatic (lignin) monomers or C_9 units. Wheat straw and Miscanthus contain both guaiacyl (G) and syringyl (S) type lignin units. To perform quantitative evaluation of interunit linkages of lignin from wheat straw and Miscanthus, it is necessary to use an internal standard that represents aromatic C_9 units in the lignin. The C_2–H_2 position of the guaiacyl unit and the $C_{2,6}$–$H_{2,6}$ positions in the syringyl unit are considered to be stable.[28] The integral of the correlation peak due to these resonances in syringyl units corresponds to twice the amount of syringyl C_9 units present. The overall amount of C_9 units present in wheat straw and Miscanthus can then be quantified by the sum of half the syringyl signal plus the guaiacyl signal. Since syringyl units are absent in pine, the amount of guaiacyl C_2–H_2 signal reflects the total number of aromatic C_9 units in lignin. In the aliphatic oxygenated region, the relative abundances of sidechains involved in the various interunit linkages were estimated from the C_α–H_α correlations to avoid possible interference from homonuclear ^{1}H–^{1}H couplings. This is except for cinnamyl alcohol end-groups, for which C_γ–H_γ correlation was used. In the aromatic/unsaturated region, $C_{2,6}$–$H_{2,6}$ correlations from G and S lignin units were used to estimate their relative abundances. Lignin aromatic units were expressed in molar percentages (H + S + G = 100).[29] The molar contents of *p*-hydroxycinnamates were calculated with respect to total lignin content (H + G + S + S′).[30,31]

2.10. Size exclusion chromatography (SEC)

Lignin solutions, 1% (w/v), were prepared in analytical-grade 1-methyl-2-pyrrolidinone (NMP). The polydispersity of dissolved lignin was determined using analytical techniques involving SEC UV-A absorbance (SEC UV-A_{300}) as previously described.[32] An Agilent 1200 series binary LC system (G1312B) equipped with DA (G1315D) detector was used. Separation was achieved with a Mixed-D column (5 mm particle size, 300 mm × 7.5 mm i.d., linear molecular mass range of 200 to 400 000 u, Polymer Laboratories) at 80 °C using a mobile phase of NMP at a flow rate of 0.5 mL min^{-1}. Absorbance of materials eluting from the column was detected at 300 nm (UV-A). Intensities were area normalized and molecular mass estimates were determined after calibration of the system with polystyrene standards. Polystyrene does not represent the geometry of the lignin molecule, based on current knowledge, but is the currently used standard for SEC calibration in the literature. Polystyrene calibrations were conducted here to confirm correct SEC system behavior and so that the data presented in this study may be compared to other published data using similar SEC systems and methods.

3. Results and discussion

This paper focuses on lignin, however full mass balances and characterization of all process streams were conducted. Detailed information on carbohydrate streams as well as hydrolysis yields, and carbohydrate characterization before and after pretreatment are presented in the ESI.†

3.1. Enhanced enzymatic hydrolysis of biomass through lignin removal and decrease in degree of crystallinity from IL pretreatment

The three feedstocks differ in carbohydrate and lignin contents as shown in Table S1.† Wheat straw and pine have comparable glucan content of ~40 wt% with Miscanthus having the highest glucan content of 48 wt%. However, pine has a high amount of mannan (~11.2 wt%) compared to that of Miscanthus and wheat straw (<3 wt%), and correspondingly lower xylan. Among these three feedstocks, pine also contains the highest amount of lignin: 32 wt% *versus* ~20 wt% for wheat straw and Miscanthus.

IL pretreatment was conducted at 120 and 160 °C on these three feedstocks. Glucan content increased in the recovered biomass with an increase in temperature for all feedstocks, due to enhanced lignin removal, whilst xylan content remained relatively constant, due to xylan loss during pretreatment (Table S1†). An increase in pretreatment temperature decreased solid recovery percentage of pretreated biomass (Table S1†). At higher temperatures, the autohydrolysis reaction is more dominant, leading to depolymerization of cellulose and hemicelluloses as evidenced by a decrease in recovered percentage of glucan and xylan at 160 °C (Fig. S3 and S4†).

All biomass samples were hydrolyzed by commercial cellulase enzymes. Untreated wheat straw, Miscanthus, and pine showed slow hydrolysis rates and low glucan digestibilities of 20, 10, and 9%, respectively. After IL pretreatment, significant enhancement of enzymatic glucan digestibility was obtained from all three feedstocks. These pretreated materials had similar hydrolysis trends but not the same efficiency (Fig. S1†). Pretreated biomass at 160 °C exhibited faster enzymatic hydrolysis with 50% of substrates hydrolyzed after 6 h (12 h for pine). The glucan digestibilities were 90% after 24 h for pretreated wheat straw and Miscanthus at 160 °C and 80% after 48 h for pretreated pine at 160 °C.

Enhanced enzymatic hydrolysis of pretreated biomass has long been the subject of extensive investigation.[33] The root cause of the enhanced enzymatic hydrolysis yields is believed to stem from many factors, such as degree of polymerization, lignin removal, degree of crystallinity, and substrate accessibility. Herein during IL pretreatment, partial lignin was solubilized and extracted in L_2. It was found that enzymatic glucan and xylan digestibilities show some correlation with lignin extraction (Fig. 2) with R^2 of 0.79 and 0.77, respectively. Moreover, the degree of crystallinity was greatly reduced after pretreatment (ESI Fig. S2†). These results suggest that enhanced enzymatic glucan release after IL pretreatment, compared to untreated, was partly due to a decrease in CrI and lignin removal.

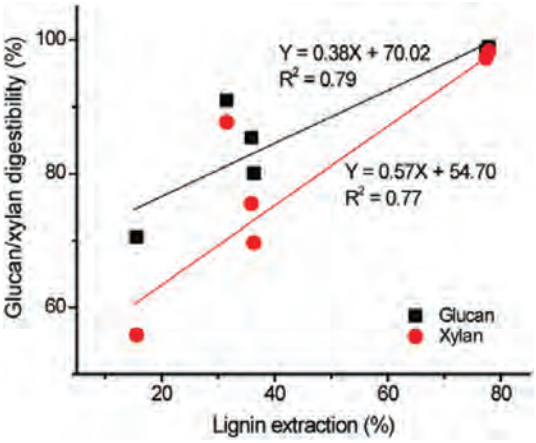

Fig. 2 Relationships between enzymatic glucan/xylan digestibility and lignin extraction efficiency. Uncertainty <5%. See Fig. S1† for enzymatic glucan digestibility profiles of pretreated biomass.

3.2. Lignin balance during biomass saccharification

During IL pretreatment, lignin was solubilized and extracted in L_2 (Fig. 1). A complete mass balance on the basis of 100 g of dry biomass, including IL pretreatment at 120 and 160 °C followed by enzymatic hydrolysis, is shown in Fig. S3 and S4.† Lignin mass balance of the biomass saccharification process is shown in Fig. 3, where lignin contents in L_2, L_3, and L_4 were normalized to initial lignin in biomass (L_1). A strong

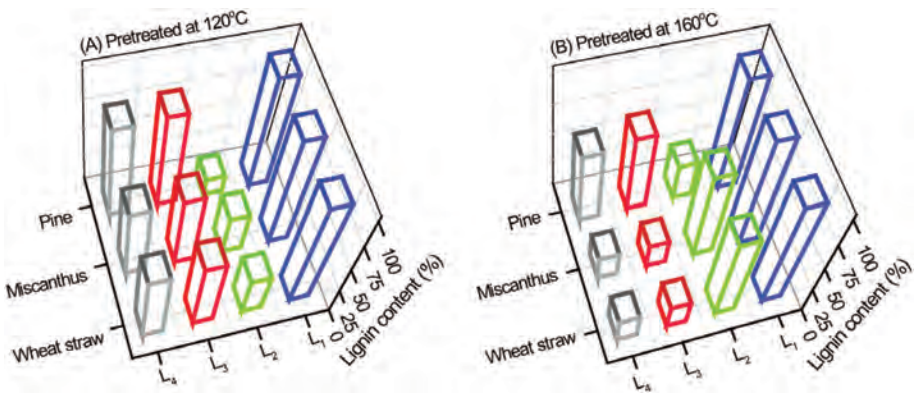

Fig. 3 Lignin mass balances from different processing streams at 120 °C (A) and 160 °C (B). L_1: lignin from untreated biomass, L_2: solubilized lignin in [C_2mim][OAc], L_3: lignin in pretreated biomass, and L_4: lignin remaining after enzymatic hydrolysis.

effect of pretreatment temperature on lignin extraction efficiency was observed in all feedstocks. At 120 °C lignin removal is ~36.3%, 35.9%, and 15.6% for wheat straw, Miscanthus, and pine, respectively. At 160 °C an approximately two-fold increase in L_2 was observed, leaving the rest of lignin in pretreated biomass, which was extracted after enzymatic hydrolysis in L_4. These results demonstrate the possibility of "tunable" lignin fractionation into different streams using IL pretreatment.

3.3. Polydispersity of different lignin streams during biomass saccharification

Elution profiles acquired by monitoring UV-A absorbance (SEC UV-A_{300}) in Fig. S5† revealed differences between L_1 of three feedstocks. Excluded ($A_{Excluded}$) and retained ($A_{Retained}$) regions are defined using the retention time of 15.5 min (u = ~46k by polystyrene calibration). The estimated molecular mass and relative area of eluted fractions are calculated and summarized in Table 1. Decreases in the ratios of the relative area ($A_{Excluded/Retained}$ ($A_{E/R}$)) of the mass peak of larger molecular mass lignin products (t < 15.5 min) to smaller molecular mass lignin products (t > 15.5 min) for L_1, are a broad gauge for depolymerization, *i.e.* an indication of the amount of material transferred from large molecular mass molecules to small. The $A_{E/R}$ of L_1 of wheat straw, Miscanthus, and pine are relatively high (*i.e.*, 4.08, 3.45, and 8.61, respectively), suggesting that L_1 consists of mainly large molecular mass materials, with pine containing the greatest proportion of larger molecular mass materials and Miscanthus the smallest.

For wheat straw, after IL pretreatment at 120 °C (Fig. 4A), lignin was solubilized and depolymerized as shown by a decrease in $A_{E/R}$ of L_2 of wheat straw at 120 °C compared to that of L_1 (Table 1). This result signified that lignin was depolymerized into lower molecular mass products, which are partly oligomers. Exploiting the limited lignin solubility of [C_2mim][OAc], water was added in L_2 causing high molecular mass lignin products in L_2 to precipitate as L_{2S}. SEC showed distinct partitioning of primarily large molecular mass material to the precipitate and primarily smaller molecular mass material remaining to the solvent. This was as evidenced by the majority of the material eluting in the excluded region for L_{2S}, and in the retained region for L_{2L}. Lignin remaining in pretreated wheat straw at 120 °C was then extracted in L_4. The elution profile of L_4 from wheat straw at 120 °C indicated that L_4 of pretreated wheat straw at 120 °C was larger than L_{2S}, suggesting that L_{2S} was depolymerized more than L_4. These data also corroborate the idea that, at this temperature, the more recalcitrant lignin that is not solvated or depolymerized by ionic liquids is the largest molecular mass lignin. Interestingly, the elution profile of L_4 is almost identical to that of EMAL, L_1, indicating that the final residue in the process retains native lignin structure.

The effect of an increase in pretreatment temperature from 120 to 160 °C for wheat straw is shown in Fig. 4A and 4B. An increase in pretreatment temperature caused $A_{E/R}$ of L_2 at 160 °C to be higher than that at 120 °C, suggesting that L_2 at 120 °C contained more smaller molecular mass lignin products. A possible reason is that at 160 °C more lignin was solvated in [C_2mim][OAc] and it was not all depolymerized. Consequently, there were some larger molecular mass lignin products, as shown by a more polydisperse elution profile in the excluded region of L_2 at 160 °C. These larger molecular mass lignin products in L_2 were readily precipitated as L_{2S}, as evidenced by a higher $A_{E/R}$ value of 1.94 from L_{2S} at 160 °C compared to 1.72 from L_{2S} at 120 °C. $A_{E/R}$ of L_{2S} of wheat straw at 160 °C was 0.13, which was higher than 0.09 from L_{2S} of wheat straw at 120 °C. At 160 °C, high molecular mass lignin was solvated in [C_2mim][OAc]. Consequently, L_{2S} of wheat straw at 160 °C contained higher levels of large molecular mass lignin products than that at 120 °C. In addition more large material was observed in L_{2L} at 160 °C than at 120 °C, again likely due to the fact that more of the larger molecular mass lignin present in the original biomass was solvated at higher temperatures. Whereas L_4 at 120 °C retained native structure, L_4 from pretreated wheat straw at 160 °C, contained more smaller molecular mass material than both L_4 at 120 °C and the original EMAL. The fact that there is more small lignin in L_4 at 160 °C than in EMAL indicates that there is a recalcitrant lignin "backbone", as shown by the data for L_4 at 120 °C, that is not solvated at 160 °C but has had either branches or end-units removed, reducing its molecular mass but not allowing it to solubilize. This has been shown elsewhere.[32] These data again highlight the importance of temperature in delignification and lignin depolymerization.

At 120 °C lignin behavior in Miscanthus is similar to wheat straw. The majority of material extracted into the L_2 stream is small. After precipitation analysis showed any large material in the L_2 stream was precipitated to L_{2S} ($A_{E/R}$ 0.06) while the majority of small material remained in solution, L_{2L} ($A_{E/R}$ 0.91). As more lignin was solvated in [C_2mim][OAc] at 160 °C, L_2 at 160 °C of Miscanthus appeared to be more polydispersed as evidenced by higher $A_{E/R}$ than that at 120 °C. The elution profile of L_{2S} of Miscanthus at 160 °C (Fig. 4D) revealed that L_{2S} at 160 °C contained higher molecular mass lignin products compared to L_{2S} at 120 °C, implying that large molecular mass lignin products in L_2 at 160 °C was readily precipitated. At 160 °C, L_4 of Miscanthus was depolymerized slightly more than that at 120 °C, but this change was not statistically significant. As with wheat straw, L_4 of Miscanthus at 120 and 160 °C is similar to L_1.

Elution profiles of pine lignin behaved differently to those of wheat straw and Miscanthus. L_2 of pine at 160 °C was more polydispersed compared to that at 120 °C. As such, $A_{E/R}$ of L_{2S} at 160 °C was higher than that at 120 °C, implying that L_{2S} at 160 °C contained larger molecular mass lignin products. Similar to the elution profiles of L_4 from wheat straw and Miscanthus, an increase in pretreatment temperature from 120 to 160 °C revealed a decrease in $A_{E/R}$ value from 1.50 to 1.41, respectively. This result suggests that some of the lignin in pine that cannot be depolymerized at 120 °C can be depolymerized 160 °C.

Table 1 Elution time and estimated molecular mass of extracted lignin extracted from ionic liquid pretreatment and enzyme hydrolysis of different feedstocks: wheat straw, Miscanthus, and pine. Molecular masses are quoted *via* polystyrene calibration

			Wheat straw								
				120 °C				160 °C			
Region	Elution time (min)	Molecular mass	L_1	L_2	L_{2L}	L_{2S}	L_4	L_2	L_{2L}	L_{2S}	L_4
Excluded	$t < 15.5$	$u > 46k$	0.80 ± 0.04	0.08 ± 0.02	0.03 ± 0.00	0.63 ± 0.01	0.81 ± 0.03	0.12 ± 0.02	0.07 ± 0.02	0.66 ± 0.00	0.75 ± 0.01
Retained	$15.5 > t$	$46k > u$	0.20 ± 0.04	0.82 ± 0.02	0.97 ± 0.04	0.37 ± 0.01	0.19 ± 0.02	0.88 ± 0.02	0.93 ± 0.02	0.34 ± 0.00	0.25 ± 0.01
$A_{Excluded/Retained}$ ($A_{E/R}$)			4.08 ± 0.86	0.09 ± 0.02	0.03 ± 0.03	1.72 ± 0.06	4.20 ± 0.52	0.13 ± 0.02	0.07 ± 0.02	1.94 ± 0.00	2.97 ± 0.16
			Miscanthus								
				120 °C				160 °C			
			L_1	L_2	L_{2L}	L_{2S}	L_4	L_2	L_{2L}	L_{2S}	L_4
Excluded	$t < 15.5$	$u > 46k$	0.78 ± 0.04	0.06 ± 0.04	0.06 ± 0.04	0.48 ± 0.02	0.77 ± 0.03	0.11 ± 0.00	0.05 ± 0.01	0.53 ± 0.04	0.75 ± 0.05
Retained	$15.5 > t$	$46k > u$	0.22 ± 0.04	0.94 ± 0.04	0.94 ± 0.04	0.52 ± 0.02	0.23 ± 0.03	0.89 ± 0.00	0.95 ± 0.01	0.47 ± 0.04	0.25 ± 0.05
$A_{Excluded/Retained}$ ($A_{E/R}$)			3.45 ± 0.57	0.06 ± 0.05	0.06 ± 0.04	0.91 ± 0.06	3.32 ± 0.44	0.12 ± 0.01	0.06 ± 0.01	1.11 ± 0.12	3.04 ± 0.66
			Pine								
				120 °C				160 °C			
			L_1	L_2	L_{2L}	L_{2S}	L_4	L_2	L_{2L}	L_{2S}	L_4
Excluded	$t < 15.5$	$u > 46k$	0.90 ± 0.01	0.09 ± 0.02	0.03 ± 0.00	0.66 ± 0.03	0.60 ± 0.02	0.17 ± 0.04	0.08 ± 0.01	0.68 ± 0.04	0.59 ± 0.04
Retained	$15.5 > t$	$46k > u$	0.10 ± 0.01	0.91 ± 0.02	0.97 ± 0.01	0.34 ± 0.02	0.40 ± 0.05	0.83 ± 0.04	0.92 ± 0.01	0.33 ± 0.05	0.41 ± 0.02
$A_{Excluded/Retained}$ ($A_{E/R}$)			8.61 ± 0.01	0.10 ± 0.03	0.03 ± 0.01	1.91 ± 0.14	1.50 ± 0.20	0.20 ± 0.04	0.08 ± 0.01	2.07 ± 0.32	1.41 ± 0.08

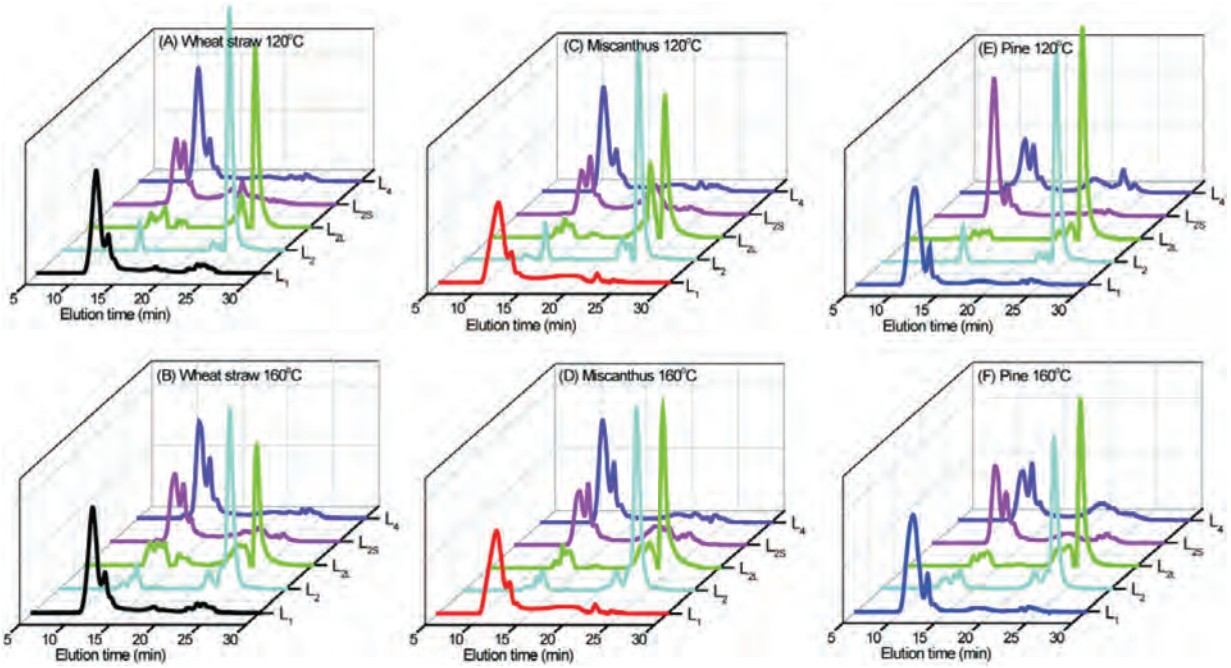

Fig. 4 Area-normalized SEC chromatograms of different lignin processing streams from pretreatment at 120 and 160 °C, followed by enzymatic hydrolysis from wheat straw (A, B), Miscanthus (C, D), Loblolly pine (E, F). SEC chromatograms were obtained using UV absorbance (λ_{300}). L_1: lignin from untreated biomass, L_2: solubilized lignin in [C_2mim][OAc], L_{2S}: precipitated solid lignin from L_2, L_{2L}: remaining lignin in the supernatant after L_{2S} precipitation, L_3: lignin in pretreated biomass, and L_4: lignin remaining after enzymatic hydrolysis. See Table 1 for relative area of excluded and retained regions.

3.4. Structural polysaccharides and lignin changes were observed by 2D HSQC

2D ^{13}C–^{1}H HSQC NMR was used to observed changes in plant cell wall chemistry before and after pretreatment, enabling observation of changes in chemical structure of lignin and polysaccharides without extraction steps. Exploiting the biomass dissolution capability of [C_2mim][OAc] for pretreatment, a small amount of [C_2mim][OAC] was added as a co-solvent, aiding complete biomass dissolution for 2D ^{13}C–^{1}H HSQC NMR.[25] The 2D HSQC spectra of wheat straw, Miscanthus, and pine before and after pretreatment at 120 °C and 160 °C are shown in Fig. S6–S8,† respectively. The common structures in these HSQC spectra correspond to the color-coded structures in Fig. S9.† The peak assignment was performed according to previously published literature[20,27,30,34–38] are shown in Table S3.† Different lignin side-chains and lignin interunit correlations are readily distinguished in the aliphatic (top row, Fig. S6–S8†) and aromatic (bottom row, Fig. S6–S8†) regions. The structural polysaccharides are shown in the anomeric region (middle row, Fig. S6–S8†). Changes in lignin structural characteristics were determined based on volume integration of HSQC spectral contour correlations (Table S5†). Fig. 5 depicts changes in lignin interunit linkages, lignin aromatic units, and levels of *p*-hydroxycinnamate. All integrals displayed less than 10% uncertainty, confirming the precision of the quantification from 2D HSQC spectra.

3.4.1. Wheat straw. *Aliphatic region*: wheat straw cell walls (Fig. S6A–C†) provide well-resolved spectra. β-Aryl ether interunit linkages (substructure A) are the major linkages in lignin. Small amounts of phenylcoumaran (substructure B), resinol (substructure C), and dibenzodioxocin (substructure D) were found in wheat straw cell walls. The β-correlation of β-O-4 was well separated into guaiacyl ($A_{\beta(G)}$) and syringyl ($A_{\beta(S)}$) types.

After IL pretreatment at 120 °C, 2D HSQC spectra of pretreated wheat straw (Fig. S6D–F†) show weaker intensities of β-aryl ethers. One possible reason was due to a partial lignin extraction during IL pretreatment at 120 °C in stream 2 (Fig. 3A). L_{2S} at 120 °C appeared to be depolymerized from SEC data and this is corroborated by a decrease in β-O-4 interunit linkages per 100 aromatic units (Fig. 5A).

The dibenzodioxocin linkages also give insight into the changing structures in lignin after IL pretreatment. In wheat straw sample, ~7.9 dibenzodioxocin linkages (per 100 aromatic units) detected in the untreated wheat straw and are completely removed in L_{2S} at 120 °C (Fig. 5A) and only a small amount was detected in L_4. The dibenzodioxocin linkages are associated with branching in lignin,[39,40] so its disappearance after IL pretreatment indicates the removal of lignin branches. This indicates that mixtures of smaller, more linear molecules are produced, comprising of a more linear lignin "backbone" and the linear branches that have been removed. A more linear molecule, with fewer bond-types, is more amenable to valorizing than a heavier, more branched molecule containing more bond-types.

Also of note is that contents of cinnamyl alcohol end-groups in L_{2S} and L_4 at 120 °C were higher than those of

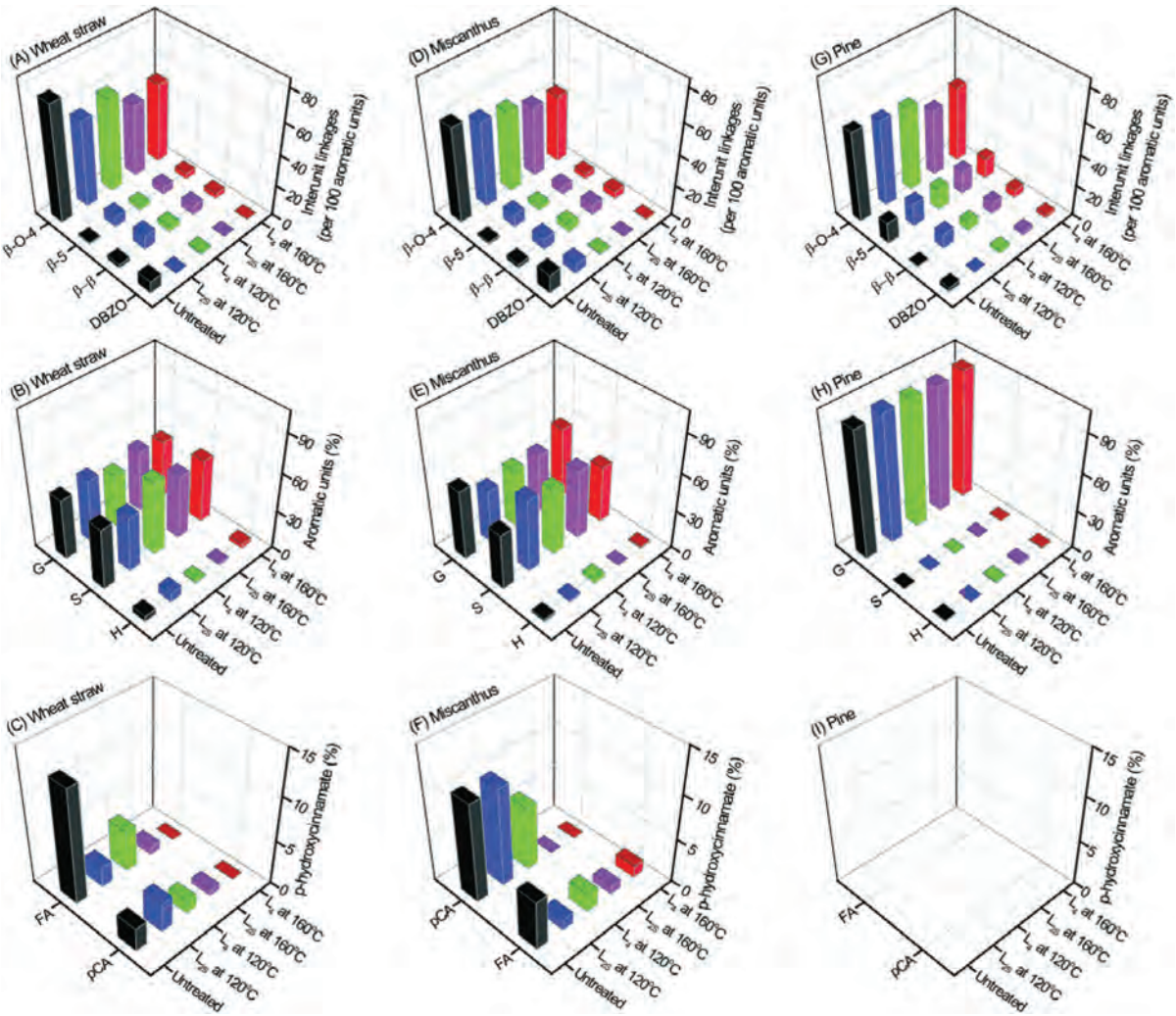

Fig. 5 Schematic diagram of changes in lignin interunit linkages [(β-O-4) β-aryl ethers, (β-5) phenylcoumarans, (β–β) resinols, and (DBZO) dibenzodioxocins], aromatic units [(G) guaiacyl, (S) syringyl, and (H) *p*-hydroxyphenyl], *p*-hydroxycinnamate contents [(FA) ferulates and (*p*CA) *p*-coumarates] of different lignin processing streams from wheat straw, Miscanthus, and pine. L_1: lignin from untreated biomass, L_{2S}: precipitated solid lignin from L_2, and L_4: lignin remaining after enzymatic hydrolysis. For clarity of presentation, It should be noted that *p*CA and FA of Miscanthus are not in the same order as those of wheat straw and pine. See Tables S4 and S5† for changes in structural characteristics of carbohydrates and lignin before and after pretreatment.

untreated wheat straw. Moreover, cinnamyl alcohol end-groups in L_4 were higher than those in L_{2S}. This corroborates with the SEC elution profiles in Fig. 4A that L_{2S} is more highly depolymerized than L_4, because an increase in depolymerization, *via* destruction of specifically the β-O-4 linkage, would result in an increase in total number of lignin molecules and "free" vinylic units (*e.g.* cinnamyl alcohol end groups).

Aromatic region: wheat straw is known to contain guaiacyl (G), syringyl (S), and *p*-hydroxyphenyl (H) type lignin units. Ferulates (FA) and *p*-coumarates (*p*CA), which are largely acylating arabinoxylans, are readily seen in the aromatic region. Untreated wheat straw contains not only G and S units, but also 2.6% *p*CA and 12.9% FA. These results are similar to previously reported values.[29] *p*CA and FA are involved in lignification, cross-coupling with lignin monomers and forming lignin-carbohydrate complexes (LCC). Relative levels of G and S units were only slightly affected by IL pretreatment regardless of processing streams and pretreatment temperatures, as shown in Fig. 5B. A significant decrease in FA in L_{2S} and L_4 at 120 °C indicated a breakage of LCC linkages during IL pretreatment at 120 °C (Fig. 5C). As pretreatment temperature increased from 120 to 160 °C, a further decrease in *p*CA and FA was observed. This implies fewer hemicelluloses conjugated with the lignin after pretreatment at higher temperatures. The HSQC spectrum of untreated wheat straw also showed a presence of a new component (T) shown in Fig. S6C.† The signal of T was analyzed previously and found to be a signal of tricin moieties,[29] which were bound to the lignin network. Further study is needed to understand functions and biosynthesis of tricin.

3.4.2. Miscanthus. *Aliphatic region*: the 2D HSQC spectra of untreated Miscanthus are shown in Fig. S7A–C.† Similar to

wheat straw, β-aryl ether interunit linkages were dominant in untreated Miscanthus. Weak cross peak intensities of phenylcoumaran, resinol, and dibenzodioxocin were observed (Fig. S7A†). The β-correlation of β-O-4 was well resolved into $A_{\beta(G)}$ and $A_{\beta(S)}$.

2D HSQC spectra of pretreated Miscanthus at 120 °C showed weaker β-aryl ether, phenylcoumaran, and resinol linkages. One reason is that at 120 °C, ~35.9% lignin was extracted from Miscanthus in the stream 2 (Fig. 3A). L_{2S} of Miscanthus at 120 °C showed a decrease in β-O-4 linkages per 100 aromatic units compared to that of untreated Miscanthus (Fig. 5D). Moreover, a significant decrease in dibenzodioxocins of L_{2S} of Miscanthus at 120 °C implied that L_{2S} was less branched compared to that of untreated Miscanthus. At the higher pretreatment temperature (160 °C), extracted solid lignins in L_{2S} and L_4 showed a higher degree of depolymerization as evidenced by a further decrease in β-O-4 linkages compared to those at 120 °C, which is in agreement with SEC elution profile in Fig. 4B and 4C. Moreover, at 160 °C dibenzodioxocins were not observed, implying that L_{2S} and L_4 at 160 °C were less branched compared to those at 120 °C. Again this is corroborated by SEC elution profiles showing a larger number of smaller molecules.

Aromatic region: Miscanthus contains S and G type lignin with H, FA and *p*CA. Unlike wheat straw, the level of *p*CA is higher than that of FA in Miscanthus,[41] as shown in a stronger *p*CA signal in untreated Miscanthus (Fig. S7G†) compared to that of wheat straw (Fig. S6G†). The level of *p*CA remained relatively unchanged (Fig. 5F), but an obvious decrease in the level of FA in the L_{2S} of Miscanthus at 120 °C suggests a cleavage of LCC linkages. Additionally, L_{2S} also contained fewer conjugated hemicelluloses. The remaining lignin, L_4, of Miscanthus at 120 °C exhibits similar trends to L_{2S}. This suggests that pretreatment at 120 °C might not be sufficient to cleave LCC linkages of Miscanthus. The levels of *p*CA and FA of L_{2S} and L_4 of Miscanthus at 160 °C were significantly lower than those at 120 °C, indicating less conjugation of hemicelluloses in the extracted L_{2S} and L_4 of Miscanthus at 160 °C.

3.4.3. Pine. *Aliphatic region*: 2D HSQC spectra of untreated pine are shown in Fig. S8A–C.† β-Aryl ether interunit linkages are the major structures of pine lignin. Phenylcoumaran, resinol, and dibenzodioxocin linkages were also detected. The β-correlation of β-O-4 ($A_{\beta(G)}$) was clearly resolved. Similar to wheat straw and Miscanthus, at 120 °C extracted lignins in L_{2S} and L_4 were depolymerized as shown by a slight decrease in β-O-4 linkages (Fig. 5G), which is in agreement with SEC elution profiles (Fig. 4E). An increase in pretreatment temperature from 120 to 160 °C did not show any statistically significant impact on cleavage of β-aryl ether and phenylcoumaran linkages. Moreover, a slight decrease in dibenzodioxocins was observed in both L_{2S} and L_4 of pretreated pine at 120 and 160 °C. No distinct changes in lignin interunit linkages from pine after pretreatment at 120 and 160 °C were observed. Pine possesses a high degree of recalcitrance[42] compared to herbaceous biomass (wheat straw and Miscanthus), which is mostly due to the more condensed nature of the lignin aromatics, such as bi-phenyls and di-phenyl ethers. Moreover, pine contains more lignin than herbaceous species. The recalcitrant nature of pine is also reflected in the lower enzymatic glucan digestibility of pretreated pine compared to those of wheat straw and Miscanthus at 120 and 160 °C (Fig. S1†). The hydrolysis rates of pretreated pine at 120 °C were also slower than that of wheat straw and Miscanthus. As pretreatment temperature increased to 160 °C, pretreated pine at 160 °C was hydrolyzed slightly faster than that at 120 °C.

The slight decrease in β-O-4 linkages even after pretreatment of pine at 160 °C in Fig. 5G is also supported by the low enzymatic digestibilities of pretreated pine (only 73% and 87% at 120 and 160 °C, respectively) compared to pretreated wheat straw and Miscanthus, and the pretreatment mass balance which shows low lignin removal after pretreatment (15.6 and 31.5% at 120 and 160 °C, respectively).

Aromatic region: the aromatic region (Fig. S8C†) shows that pine lignin is a G type lignin. No *p*CA and FA were detected in pine. Levels of *p*CA and FA exist in such a small degree and are not typically detectable by NMR.

4. Conclusion

Lignin depolymerization is one of the major obstacles to fully valorizing lignin. Depolymerization of lignin is not an easy task, as there is an associated repolymerization and condensation. Our findings reveal that IL pretreatment using a non-toxic and recyclable ionic liquid, [C_2mim][OAc], yields pretreated substrates with a low degree of cellulose crystallinity and low degree of acetylation. This enables the pretreated substrates to be significantly more susceptible to enzymatic hydrolysis than untreated biomass. Importantly, using this IL pretreatment method no condensed structures were observed in extracted lignin from the feedstocks studied under current conditions. In addition, lignin extraction was customizable by tuning the pretreatment conditions: extracted lignin during pretreatment (L_{2S}) and after enzymatic hydrolysis (L_4) with larger molecular weight at lower severity conditions, as well as predominantly smaller molecular mass lignin products in L_{2L} in higher severity conditions. L_{2S} and L_4 from all three feedstocks were shown to be depolymerized by varying degrees and levels of β-O-4 linkages per 100 aromatic units of L_{2S} and L_4 were reduced compared to those in the initial biomass. This study shows the potential of tuning IL pretreatment process conditions to obtain particular lignin structures and molecular sizes in different streams for lignin valorization.

Acknowledgements

This work was performed as part of a collaboration program between JBEI and Total. Noppadon Sathitsuksanoh's and Anthe George's work in this program is funded by Total. Angelique Chanal, Vineet Rajgarhia, Laurent Fourage and Henri

Strub, Total New Energies – R&D, are acknowledged for their contribution to this collaborative program. The portion of the work conducted by the Joint BioEnergy Institute was supported by the Office of Science, Office of Biological and Environmental Research, of the U.S. DOE under Contract no. DE-AC02-05CH11231.

References

1 L. R. Lynd, M. S. Laser, D. Bransby, B. E. Dale, B. Davison, R. Hamilton, M. Himmel, M. Keller, J. D. McMillan, J. Sheehan and C. E. Wyman, *Nat. Biotechnol.*, 2008, **26**, 169–172.
2 N. Sathitsuksanoh, Z. Zhu, N. Templeton, J. A. Rollin, S. P. Harvey and Y.-H. P. Zhang, *Ind. Eng. Chem. Res.*, 2009, **48**, 6441–6447.
3 N. Sathitsuksanoh, Z. Zhu, T. Ho, M. Bai and Y.-H. P. Zhang, *Bioresour. Technol.*, 2010, **101**, 4926–4929.
4 N. Sathitsuksanoh, Z. Zhu, S. Wi and Y.-H. P. Zhang, *Biotechnol. Bioeng.*, 2011, **108**, 521–529.
5 Y. Kim, N. S. Mosier, M. R. Ladisch, V. Ramesh Pallapolu, Y. Y. Lee, R. Garlock, V. Balan, B. E. Dale, B. S. Donohoe, T. B. Vinzant, R. T. Elander, M. Falls, R. Sierra, M. T. Holtzapple, J. Shi, M. A. Ebrik, T. Redmond, B. Yang, C. E. Wyman and R. E. Warner, *Bioresour. Technol.*, 2011, **102**, 11089–11096.
6 N. Mosier, C. Wyman, B. Dale, R. Elander, Y. Lee, M. Holtzapple and M. Ladisch, *Bioresour. Tech.*, 2005, **96**, 673–686.
7 N. Sathitsuksanoh, Z. Zhu and Y.-H. P. Zhang, *Bioresour. Tech.*, 2012, **117**, 228–233.
8 Ö. Çetinkol, D. Dibble, G. Cheng, M. Kent, B. Knierim, M. Auer, D. Wemmer, J. Pelton, Y. Melnichenko and J. Ralph, *Biofuels*, 2010, **1**, 33–46.
9 C. Li, B. Knierim, C. Manisseri, R. Arora, H. V. Scheller, M. Auer, K. P. Vogel, B. A. Simmons and S. Singh, *Bioresour. Technol.*, 2010, **101**, 4900–4906.
10 S. H. Lee, T. V. Doherty, R. J. Linhardt and J. S. Dordick, *Biotechnol. Bioeng.*, 2008, **102**, 1368–1376.
11 G. Bokinsky, P. P. Peralta-Yahya, A. George, B. M. Holmes, E. J. Steen, J. Dietrich, T. S. Lee, D. Tullman-Ercek, C. A. Voigt and B. A. Simmons, *PNAS*, 2011, **108**, 19949–19954.
12 D. Groff, A. George, N. Sun, N. Sathitsuksanoh, G. Bokinsky, B. A. Simmons, B. M. Holmes and J. D. Keasling, *Green Chem.*, 2013, **15**, 1264–1267.
13 J. Shi, J. Gladden, N. Sathitsuksanoh, P. Kambam, L. Sandavol, D. Mitra, S. Zhang, S. Singer, A. George, B. Simmons and S. Singh, *Green Chem.*, 2013, **15**, 2579–2589.
14 R. Wooley, M. Ruth, D. Glassner and J. Sheehan, *Biotechnol. Prog.*, 1999, **15**, 794–803.
15 J. Li, G. Henriksson and G. Gellerstedt, *Bioresour. Technol.*, 2007, **98**, 3061–3068.
16 M. J. Selig, S. Viamajala, S. R. Decker, M. P. Tucker, M. E. Himmel and T. B. Vinzant, *Biotechnol. Prog.*, 2007, **23**, 1333–1339.
17 P. Sannigrahi, D. H. Kim, S. Jung and A. Ragauskas, *Energy Environ. Sci.*, 2011, **4**, 1306–1310.
18 D. J. Yelle, P. Kaparaju, C. G. Hunt, K. Hirth, H. Kim, J. Ralph and C. Felby, *BioEnergy Res.*, 2013, **6**, 211–221.
19 G. W. Huber, S. Iborra and A. Corma, *Chem. Rev.*, 2006, **106**, 4044–4098.
20 H. Kim and J. Ralph, *Org. Biomol. Chem.*, 2010, **8**, 576–591.
21 G. Moxley and Y.-H. P. Zhang, *Energy Fuels*, 2007, **21**, 3684–3688.
22 A. Sluiter, B. Hames, R. Ruiz, C. Scarlata, J. Sluiter, D. Templeton and D. Crocker, in Technical Report. NREL/TP-510-42618, 2011.
23 L. Segal, J. Creely, A. Martin Jr. and C. Conrad, *Text. Res. J.*, 1959, **29**, 786.
24 S. D. Mansfield, H. Kim, F. Lu and J. Ralph, *Nat. Protoc.*, 2012, **7**, 1579–1589.
25 K. Cheng, H. Sorek, H. Zimmermann, D. E. Wemmer and M. Pauly, *Anal. Chem.*, 2013, **85**, 3213–3221.
26 S. Heikkinen, M. M. Toikka, P. T. Karhunen and I. A. Kilpeläinen, *J. Am. Chem. Soc.*, 2003, **125**, 4362–4367.
27 D. J. Yelle, J. Ralph and C. R. Frihart, *Magn. Reson. Chem.*, 2008, **46**, 508–517.
28 M. Sette, R. Wechselberger and C. Crestini, *Chem.–Eur. J.*, 2011, **17**, 9529–9535.
29 J. C. Del Río, J. Rencoret, P. Prinsen, A. T. Martínez, J. Ralph and A. Gutiérrez, *J. Agric. Food Chem.*, 2012, **60**, 5922–5935.
30 J. Rencoret, G. Marques, A. Gutiérrez, L. Nieto, J. I. Santos, J. Jiménez-Barbero, Á. T. Martínez and J. C. del Río, *Holzforschung*, 2009, **63**, 691–698.
31 J. Rencoret, G. Marques, A. Gutiérrez, L. Nieto, J. Jiménez-Barbero, Á. T. Martínez and J. C. del Río, *Ind. Crops Prod.*, 2009, **30**, 137–143.
32 A. George, K. Tran, T. J. Morgan, P. I. Benke, C. Berrueco, E. Lorente, B. C. Wu, J. D. Keasling, B. A. Simmons and B. M. Holmes, *Green Chem.*, 2011, **13**, 3375–3385.
33 Y.-H. P. Zhang and L. R. Lynd, *Biotechnol. Bioeng.*, 2004, **88**, 797–824.
34 M. Bunzel and J. Ralph, *J. Agric. Food Chem.*, 2006, **54**, 8352–8361.
35 D. Ibarra, M. I. Chávez, J. Rencoret, J. C. Del Río, A. Gutiérrez, J. Romero, S. Camarero, M. J. Martínez, J. Jiménez-Barbero and Á. T. Martínez, *Holzforschung*, 2007, **61**, 634–646.
36 D. Ibarra, M. I. Chávez, J. Rencoret, J. C. Del Río, A. Gutiérrez, J. Romero, S. Camarero, M. J. Martínez, J. Jiménez-Barbero and Á. T. Martínez, *J. Agric. Food Chem.*, 2007, **55**, 3477–3490.
37 H. Kim, J. Ralph and T. Akiyama, *BioEnergy Res.*, 2008, **1**, 56–66.

38 A. Thygesen, J. Oddershede, H. Lilholt, A. B. Thomsen and K. Stahl, *Cellulose*, 2005, **12**, 563–576.
39 D. S. Argyropoulos, L. Jurasek, L. Krištofová, Z. Xia, Y. Sun and E. Paluš, *J. Agric. Food Chem.*, 2002, **50**, 658–666.
40 E. A. Capanema, M. Y. Balakshin and J. F. Kadla, *J. Agric. Food Chem.*, 2004, **52**, 1850–1860.
41 Z. Liu, S. Padmanabhan, K. Cheng, P. Schwyter, M. Pauly, A. T. Bell and J. M. Prausnitz, *Bioresour. Technol.*, 2013, **135**, 23–29.
42 K. M. Torr, K. T. Love, O. P. Cetinkol, L. A. Donaldson, A. George, B. M. Holmes and B. A. Simmons, *Green Chem.*, 2012, **14**, 778–787.